ARTICLE IN PRESS

Available online at www.sciencedirect.com
SCIENCE DIRECT®

Chemical Physics xxx (2004) xxx–xxx

Chemical Physics

www.elsevier.com/locate/chemphys

Electron–phonon interaction in absorption and photoluminescence spectra of quantum dots

T.O. Cheche [a,b,*,1], M.C. Chang [b], S.H. Lin [c]

[a] *Faculty of Physics, University of Bucharest, P.O. Box 11, Magurele, Bucharest, Romania*
[b] *Department of Physics, National Taiwan Normal University, Taipei, Taiwan*
[c] *Institute of Atomic and Molecular Sciences, Academia Sinica, Taipei, Taiwan*

Received 21 May 2004; accepted 31 August 2004

Abstract

Optical absorption of quantum dots is investigated using the adiabatic approach, in which a Fröhlich-type interaction between electron–hole pair and longitudinal optical phonons has been assumed. The role of the finite barrier potentials in predicting the magnitude of the Huang–Rhys factors is considered. For the small GaAs/AlAs quantum dots, the Huang–Rhys factors are found to be larger than those in the bulk phase by one to two orders of magnitude. The absorption and photoluminescence spectra of such nanostructures are analyzed.

Keywords: Optical absorption; Photoluminescence; Quantum dot

1. Introduction

Theoretically, the response of one or several electron–hole pairs (EHPs) is often invoked to explain the optical spectra of semiconductor quantum dots (QDs). The adiabatic approximation is frequently used when the electron–phonon coupling is taken into account. It is widely accepted that a strong quantum confinement of the electron or a strong electron–phonon interaction, which result in increasing of kinetic energy of the electrons, are circumstances which justify an adiabatic treatment (see, e.g. [1]). The ineffectiveness of the electron–phonon coupling implies weak phonon-induced mixing between the energy levels of QD. On the other hand, when the level spacing becomes comparable with the optical phonon energy (see, e.g. [2]), the phonon mixing of the EHP states becomes important. In this case, the phonon-assisted absorption is a more probable process and a nonadiabatic approach is demanded. Such a nonadiabatic treatment is used to explain the discrepancy between the large values of Huang–Rhys factors found experimentally and the smaller ones predicted by adiabatic treatment [3]. On the other hand, for small QDs there are experimental reports of large values of Huang–Rhys factors (by two orders of magnitude larger than in the bulk phase). In such cases the mixing effect induced by phonons becomes less important as the inter-level energy is usually much larger than the LO phonon energy and the optical processes are adiabatic. The problem of Huang–Rhys factor of small QDs, where nonadiabatic effects are expected to be insignificant and the adiabatic approach appropriate, is addressed in this paper. We provide an explanation for the experimental observation of increasing Huang–Rhys factor with decreasing of QD radius.

We use a simple model to describe the interaction between photon, EHP, and phonon. Thus, to investigate

* Corresponding author. Tel.: +886 2 293 17515x174; fax: +886 2 293 26408.
E-mail address: cheche@home.phy.ntnu.edu.tw (T.O. Cheche).
[1] Tel.: +4013309873; fax: +4014208625.

0301-0104/$ - see front matter © 2004 Published by Elsevier B.V.
doi:10.1016/j.chemphys.2004.08.018

the phonon-assisted optical processes, we consider the limit of low excitation intensities and work within the framework of the adiabatic Huang–Rhys-type treatment [4]. To model small GaAs microcrystallites embedded in AlAs matrix, we choose spherical symmetry and finite confinement potentials for both electron and hole, isotropic and parabolic electron and hole bands [5,6], and consider the effective mass approximation and pure EHPs. Moreover, in the case of small QDs that we analyze, the Coulomb electron–hole interaction can be considered as a perturbation to the confinement potential [7], which can be neglected in the zeroth order approximation. Though simple, the adopted QD model is accurate enough for the considered application, as we shall argue. Though the calculation of the optical spectra is common in the literature [8], we present a procedure of deriving the linear absorption coefficient, which can be used for both adiabatic and nonadiabatic cases (the latter is investigated in [9]). Then, the optical selection rules, the Huang–Rhys factors, the spectra of absorption and photoluminescence (PL) are obtained for spherical QDs. The use of the adiabatic approach is justified and the range of its validity discussed. We find that, for small QDs, the adiabatic treatment is able to predict values of Huang–Rhys factors larger than in the bulk phase by one to two orders of magnitude.

1.1. Optical absorption coefficient

To describe the confined EHP, we use the Hamiltonian

$$H = H_{\mathrm{p}} + H_{\mathrm{ph}} + H_{\mathrm{p-ph}} \equiv \sum_f \varepsilon_f B_f^+ B_f + \sum_{\boldsymbol{q}} \hbar\omega_{\boldsymbol{q}} b_{\boldsymbol{q}}^+ b_{\boldsymbol{q}} + \sum_{\boldsymbol{q},f} M_{\boldsymbol{q}}^f B_f^+ B_f (b_{\boldsymbol{q}} + b_{-\mathbf{q}}^+), \tag{1}$$

in which f labels the EHP eigenstate, $H_{\mathrm{p}}|f\rangle = E_f|f\rangle$, $\omega_{\boldsymbol{q}}$ is the frequency of the mode with the wavevector $\boldsymbol{q}$, B_f^+ (B_f) and b_{-q}^+ (b_q) are the creation (annihilation) operators of EHP and phonon, respectively, and $M_{\boldsymbol{q}}^f$ is the EHP–phonon coupling. The EHPs are considered as bosons, a valid approximation in the dilute limit. The radiation field is modeled as a single mode of linearly polarized plane wave. In the limit of linear response theory and long-wave approximation, the semi-classical EHP-field interaction can be written as [10,11] $H_{\mathrm{p-F}} = 2eF_0(m_0\omega)^{-1}[\sum_{f\neq 0}\langle 0|\boldsymbol{\varepsilon}\cdot\mathbf{P}|f\rangle B_f + \mathrm{h.c.}]\sin\omega t$, with m_0, e the mass and the charge of electron, $\boldsymbol{\varepsilon}$, ω, F_0, the polarization vector, frequency, and amplitude of light wave, and $\mathbf{P} \equiv \sum_i \boldsymbol{p}_i$ the total electronic momentum (with $\boldsymbol{p}_i$ the electron momentum). Initially, the electrons are in the ground electronic state $|0\rangle$ (EHP vacuum state) and the phonons are at thermal equilibrium. Applying the Fermi Golden Rule to the eigenstates of the system and using the algebra of bosonic operators, the linear one-EHP absorption coefficient may be written as

$$\alpha(\omega) = \frac{2\pi e^2}{ncm_0^2\hbar\omega V_0}\int_{-\infty}^{\infty} \mathrm{d}t\exp(\mathrm{i}\omega t)\sum_{f\neq 0} D_f\langle B_f(t)B_f^+\rangle, \tag{2}$$

where V_0 is the volume of the absorptive system, c the speed of light in vacuum, n the refractive index, $D_f \equiv |\langle 0|(\boldsymbol{\varepsilon}\cdot\mathbf{P})|f\rangle|^2$, $\langle B_f(t)B_f^+\rangle = \langle 0|\langle \exp(\mathrm{i}tH/\hbar)B_f\exp(-\mathrm{i}tH/\hbar)B_f^+\rangle_0|0\rangle$, and $\langle\cdots\rangle_0 \equiv \mathrm{Tr}[\rho_0\cdots]$ the trace over the phononic modes with ρ_0 the equilibrium density matrix of phonons. To solve Eq. (2), we introduce the time evolution operator, $U(t) \equiv \exp(\mathrm{i}tH_0/\hbar)\exp(-\mathrm{i}tH/\hbar)$, with $H_0 = H_{\mathrm{p}} + H_{\mathrm{ph}}$ and obtain $\langle \tilde{B}_f(t)B_f^+\rangle_0 = \langle 0|B_f\langle U(t)\rangle_0 B_f^+|0\rangle = \langle 0|B_f\langle \hat{T}\exp[-\mathrm{i}\int_0^t \mathrm{d}t_1\tilde{V}(t_1)/\hbar]\rangle_0 B_f^+|0\rangle$, where $\hat{T}$ is the time-ordered operator, and $\tilde{V}(t) \equiv \exp(\mathrm{i}tH_0/\hbar)H_{\mathrm{p-ph}}\exp(-\mathrm{i}tH_0/\hbar)$. With the usual expansion of the time evolution operator [8a] and the Wick's theorem for bosons, Eq. (2), which assumes a linear coupling, can be resumed. In the framework of the Einstein model ($\omega_{\boldsymbol{q}} \to \omega_0$), the *bosonic* Green's function of Eq. (2) yields a form similar to the well-known adiabatic spectral function for *fermionic* carriers [4,5,8a]

$$\alpha(\omega) = \frac{4\pi^2 e^2}{ncm_0^2\hbar\omega V_0}\sum_{f\neq 0}\left\{D_f\exp[-g_f(2\overline{N}+1)] \times \sum_{n=-\infty}^{\infty} I_n\left(g_f\sqrt{\overline{N}(\overline{N}+1)}\right)\exp(n\beta\hbar\omega_0/2) \times \delta(\omega - \omega_f + \Delta_f - n\omega_0)\right\}, \tag{3}$$

where I_n are the modified Bessel functions, $\Delta_f = \omega_0\sum_{\boldsymbol{q}}(|M_{\boldsymbol{q}}^f|\hbar^{-1}\omega_0^{-1})^2 \equiv \omega_0 g_f$ is the phononic induced renormalization of EHP energy, and g_f is the Huang–Rhys factor. However, this similarity is to be expected for an adiabatic treatment, as long as the EHP model adopted by us does not involve electron–hole interaction. The relative intensity of the absorption lines is given by the coefficients of Dirac delta functions. Eq. (3) assumes the form reported in [5] and, in addition, may be used to estimate the *absolute value* of the absorption coefficient.

1.2. Quantum dot model

Within the effective mass approximation, a spherical model is considered for the case of size-quantized energies of QD (or equivalently, QD with dimensions smaller than its corresponding exciton Bohr radius) [7]. Such a case is suitable for an adiabatic treatment as long as a typical Coulomb term, responsible of the excitonic effect, $e^2/(4\pi\kappa\varepsilon_0 r_{\mathrm{eh}})$ (κ the vacuum dielectric permittivity, ε_0 the static relative dielectric permittivity, and r_{eh} the electron–hole distance) has an energy of the order of longitudinal optical (LO) phonons.

The confinement potential energy is $V_{\mathrm{e}}(r_{\mathrm{e}}) = 0$ for $r_{\mathrm{e}} \in [0, R_0]$, and $V_{\mathrm{e}}(r_{\mathrm{e}}) = V_{0\mathrm{e}}$ for $r_{\mathrm{e}} > R_0$ (similar equation

is written for holes by replacing r_e by r_h); R_0 is the QD radius. The envelope wave function is $\varphi_{nlm}(\boldsymbol{r}) = R_{nl}(r)Y_{lm}(\theta,\varphi)$, where $R_{nl}(r)$ is the radial and $Y_{lm}(\theta,\varphi)$ the spherical harmonics function. Generally, the LO phonons are considered as the main contributors to the electron–phonon interaction in polar semiconductors. An important aspect is that, by choosing finite confinement potentials for both electrons and holes, a *non-vanishing* EHP–phonon interaction is obtained. The EHP state may be written as $|f\rangle \to |\varphi_{ab}\rangle = \int \mathrm{d}\boldsymbol{r}_e\,\mathrm{d}\boldsymbol{r}_h \varphi_a(\boldsymbol{r}_e)\varphi_b(\boldsymbol{r}_h)a_e^{c+}a_h^v|0\rangle$, where $a_e^{c+}(a_h^v)$ are the creation (annihilation) operator of an electron in the conduction band at $\boldsymbol{r}_e$ (valence band at $\boldsymbol{r}_h$) and $a(b)$ holds for the set of quantum numbers n_e, l_e, m_e (n_h, l_h, m_h) of electrons (holes). The optical selection rules are determined by the matrix element $\langle f|\boldsymbol{\varepsilon}\cdot\boldsymbol{P}|0\rangle$ of Eq. (2). Using the pure EHPs eigenstates and an appropriate definition of the momentum [12], $\mathbf{P} = \mathbf{p}_{cv}^0 \int \mathrm{d}\boldsymbol{R} a_{\boldsymbol{R}}^{c+}a_{\boldsymbol{R}}^v + \text{h.c.}$, where $\boldsymbol{p}_{cv}^0$ is the momentum matrix element between the valence-band and the conduction-band at the Γ point and $\boldsymbol{R}$ integrates over unit cells, one obtains $\langle\varphi_{ab}|\mathbf{P}|0\rangle = \mathbf{p}_{cv}^0\delta_{l_el_h}\delta_{m_em_h}\int_0^\infty \mathrm{d}r\, r^2 R_{n_el_e}(r)R_{n_hl_h}(r) \equiv \boldsymbol{p}_{cv}^0\delta_{m_em_h}A_{n_en_hl}$, with $l_e = l_h = l$ (see also [7]). Thus, the optical selection rule requires $l_e = l_h$. We model the electron–phonon interaction by the Fröhlich interaction between electrons and dispersionless bulk LO phonons, which is an acceptable approach for QD with high geometrical symmetry, where the interface modes are usually weak [5,13]. Within the pure-EHP approximation the EHP–phonon interaction reads

$$\begin{aligned} M_{\boldsymbol{q}}^f \to{}& V_0^{-1/2} f_0 q^{-1} \\ &\times \int \mathrm{d}\boldsymbol{r}_e\,\mathrm{d}\boldsymbol{r}_h \varphi_a^*(\boldsymbol{r}_e)\varphi_b^*(\boldsymbol{r}_h)\varphi_a(\boldsymbol{r}_e)\varphi_b(\boldsymbol{r}_h) \\ &\times [\exp(\mathrm{i}\boldsymbol{q}\boldsymbol{r}_e) - \exp(\mathrm{i}\boldsymbol{q}\boldsymbol{r}_h)], \end{aligned} \tag{4a}$$

which for spherical QDs becomes

$$\begin{aligned} M_{\boldsymbol{q}}^f \to M_{\boldsymbol{q}}^{ab} &= V_0^{-1/2} f_0 q^{-1} \\ &\times \int_0^\infty \mathrm{d}r\, r^2 \left[R_{n_el}(r)^2 - R_{n_hl}(r)^2\right] Q_{lm}(q,r) \\ &\equiv V_0^{-1/2} f_0 q^{-1} v_{\boldsymbol{q}}^{ab}, \end{aligned} \tag{4b}$$

where $f_0 = \sqrt{2\pi\hbar\omega_0 e^2(\varepsilon_\infty^{-1} - \varepsilon_0^{-1})\kappa^{-1}}$ is the Fröhlich coupling constant, ω_0 is the LO phonon frequency, and $Q_{lm}(q,r) \equiv \int \mathrm{d}\Omega Y_l^{m*}(\Omega)Y_l^m(\Omega)\exp(\mathrm{i}\boldsymbol{q}\boldsymbol{r}) = \sum_{l'=0}^{2l} i^{l'}(2l'+1)\, j_{l'}(qr)\langle l'l00|l0\rangle\langle l'l0m|lm\rangle$. $j_{l'}(x)$ are the spherical Bessel functions, and $\langle\cdots|\cdot\cdot\rangle$ are the Clebsch–Gordan coefficients. The last equality is obtained by using the expansion of plane waves, $\exp(\mathrm{i}\boldsymbol{q}\boldsymbol{r}) = \sum_{l'=0}^\infty (2l'+1) i^{l'} j_{l'}(qr) P_{l'}(\cos\theta)$, the addition theorem of the spherical harmonics to expand the Legendre polynomials $P_{l'}(\cos\theta)$, and the integration of three spherical harmonics over the solid angle. The Huang–Rhys factors corresponding to the state $|\varphi_{ab}\rangle$ are obtained from $\sum_{\boldsymbol{q}}|M_{\boldsymbol{q}}^{ab}|^2 \to f_0^2(2\pi^2)^{-1}\int_0^\infty \mathrm{d}q|v_{\boldsymbol{q}}^{ab}|^2$ by manipulating the spherical and modified spherical Bessel functions contained in the radial functions R_{nl}. After averaging over polarization directions, one obtains a factor 1/3 and therefore $D_f \to |\boldsymbol{p}_{cv}^0|^2 A_{n_en_hl}^2/3$ in Eq. (3).

2. Application and discussions

Though simple, the pure EHP model can pass certain tests concerning its accuracy in describing the spherical QDs. Thus, the GaAs conduction band shift induced by the strains when a GaAs sphere is embedded in AlAs is insignificant as the two semiconductors are lattice-matched (less than 10 meV, see [14]). That allows, in a first approximation, neglecting the strain effects in such semiconductor heterostructures. Also, comparing with results from [6], where one uses finite potential barrier to obtain the excitonic states, the EHP model slightly overestimates the values of energy levels (for example, less than 50 meV at $R_0 = 25$ Å for the first excitonic state). Regarding the band structure of GaAs/AlAS heterostructures, the interplay of the three lowest minima Γ, L and X for GaAs and AlAs yields a spatial confinement only for the Γ electrons (see e.g. [15]) and the energy gap is dictated by the Γ minimum. On the other hand, as reported in [16], the complexity of valence band structure and the band mixing effects become less significant for smaller spherical QDs and a one-band calculation of the energy structure is a satisfactory approximation.

Compared to [17], which also considers finite confinement potentials (and, in addition, excitonic and image charge effects) to describe spherical quantum dots embedded in a matrix, the present model takes into account the difference in the effective masses between the nanosphere and its surroundings. Following [18], the expression of orthonormalized $R_{nl}(r)$ and the secular equation of energy are as follows:

$$\begin{aligned} R_{nl}(r) = {}& \sqrt{\frac{2}{R_0^3}}\left[j_l^2(x)k_{l-1}(y)k_{l+1}(y) - k_l^2(y)j_{l-1}(x)j_{l+1}(x)\right] \\ &\times \begin{cases} k_l(y)j_l(xr/R_0), & r < R_0, \\ j_l(y)k_l(xr/R_0), & r < R_0, \end{cases} \end{aligned} \tag{5a}$$

$$m_2 x k_l(y) j_l'(x) = m_1 y j_l(x) k_l'(y), \tag{5b}$$

where $x = R_0\sqrt{(2m_1E_{n,l})/\hbar^2}$, $y = R_0\sqrt{(2m_2(V_0^c - E_{n,l}))/\hbar^2}$, k_l the modified spherical Bessel functions, m_1 (m_2) the effective mass in the dot (surrounding medium), V_0^c the band offset of the carriers, and n, $l \to n_e$, l_e or n_h, l_h for electron and hole, respectively. For GaAs microcrystallites embedded in AlAs matrix, the compound addressed in our application, we use the parameters of material from [6]: the GaAs energy gap $E_g = 1.5177$ eV, the GaAs (AlAs) electron effective mass $m_e/m_0 = 0.0665$ ($m_e/m_0 = 0.124$), the hole effective mass $m_h/m_0 = 0.45$ ($m_h/m_0 = 0.5$), the conduction band offset

$V_0^e = 0.968$ eV, and the valence band offset $V_0^h = 0.6543$ eV. The energy spectrum is obtained from Eq. (5b), and the EHP energy $E_{n_e,l_e;n_h,l_h} = E_g + E_{n_e,l_e} + E_{n_h,l_h}$ is computed as a function of the QD radius and shown in Fig. 1. Some particular levels are labeled by the set of quantum numbers, $(n_e,l_e;n_h,\ l_h)$ as follows: $A_0 \rightarrow (1,0;1,0)$, $B \rightarrow (1,0;1,1)$, $C \rightarrow (1,0;1,2)$, $D_0 \rightarrow (1,0;2,0)$, $E \rightarrow (1,1;1,0)$, $F \rightarrow (1,0;2,1)$, $G_0 \rightarrow (1,1;1,1)$.Based on the distribution of energy levels and taking into account the exciton Bohr radius (larger than 100 Å), we consider $R_0 = 50$ Å as a reasonable upper-limit for our approach. Possible phonon mixing effect could manifest starting with $R_0 \approx 23$ Å (see the ellipse mark at Fig. 1), between the optically active level G_0 and the dark level F. But, the phonon-assisted transition between G_0 and D_0 is improbable (at least in the low temperature limit) because $(E_E - E_{D_0})/\hbar\omega_0 = 3.37$ (the LO phonon energy $\hbar\omega_0 = 36.2$ meV). For the first two optically active levels, the adiabatic treatment is safe for $R_0 < 22$ Å and may be accepted as satisfactory for $R_0 < 32$ Å, beyond which the C level appears.

The Huang–Rhys factors of the optically active levels may be obtained with

$$g_{n_e,l,m;n_h,l,m} = \frac{f_0^2}{2\pi^2\hbar^2\omega_0^2}\int_0^\infty\int_0^\infty \mathrm{d}r\mathrm{d}r' r^2 r'^2 \left[R_{n_e l}(r)^2 - R_{n_h l}(r)^2\right] \times \left[R_{n_e l}(r')^2 - R_{n_h l}(r')^2\right]\int_0^\infty \mathrm{d}q\, Q_{lm}(q,r)Q_{lm}(-q,r'). \quad (6)$$

However, extension of the definition of v_q^{ab} from Eq. (4b) to dark levels immediately allows an expression to be obtained for such levels as well. Fig. 2 summarizes our calculated Huang–Rhys factors for the first two optically active levels. The values obtained are larger than those predicted for the GaAs *bulk* excitons, 0.0079 in [5]. In the extreme limit of small radius (10 Å), our model yields values which are by two orders of magnitude larger than those for the bulk, but this result must be considered with reservation because the effective mass approximation may become questionable at such small dimensions. We ascribe these large values of Huang–Rhys factors for the small spherical QDs as the result of considering finite potential barriers. Given the charge distribution of an electron (or a hole) in the QD, the Huang–Rhys factor is related to the difference between the form factors of electron and hole (see Eq. (4a)). For an infinite potential, electrons and holes have a zero charge separation, the same form factor, and the EHP–phonon coupling vanishes. By choosing finite barriers, one obtains a charge separation even for the first EHP state as seen in Fig. 3, where the charge density, $\rho(r) \propto r^2 R_{nl}(r)^2$, with $n,l \rightarrow n_{e,h} = 1$, $l_{e,h} = 0$, is shown. Besides this charge separation, the other factor involved in the form factors responsible for the increased Huang–Rhys in small QDs is the spatial confinement of the envelope wave function [19]. In their earlier calculation, Nomura and Kobayashi [5] used an infinite potential and a valence-band mixing treatment, and obtained within an excitonic model a Huang–Rhys factor of the same order of magnitude (but smaller) than for the bulk; a similar behavior of increasing Huang–Rhys factor with decreasing QD radius is obtained. Large Huang–Rhys factor are reported from measurements in small QDs, where the nonadiabatic effect is expected to be insignificant and, consequently, the excitonic effect small. Thus, for our semiconductor compound, values larger by two orders of magnitude than for the bulk are reported in [20], where localized EHPs by quantum wells-QDs intermediate states in GaAs/AlAs superlattices are analyzed. For *self-assembled* InAs/GaAs QDs, where the strain, band mixing and shape effects cannot be neglected, and the simple spherical QD model be-

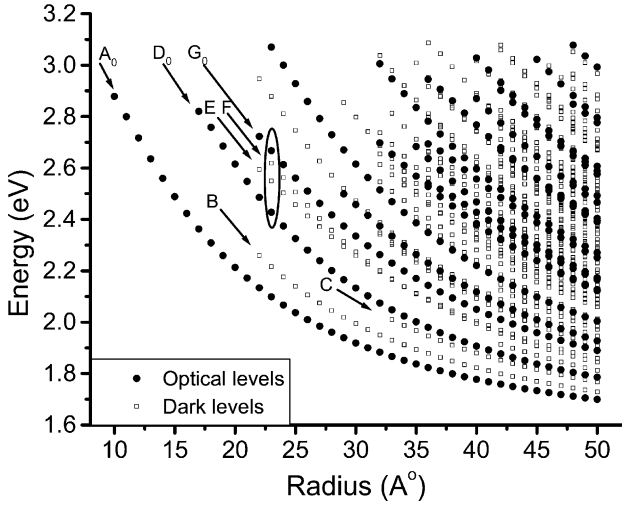

Fig. 1. The energy spectrum of small spherical GaAs/AlAs QDs within the adopted model.

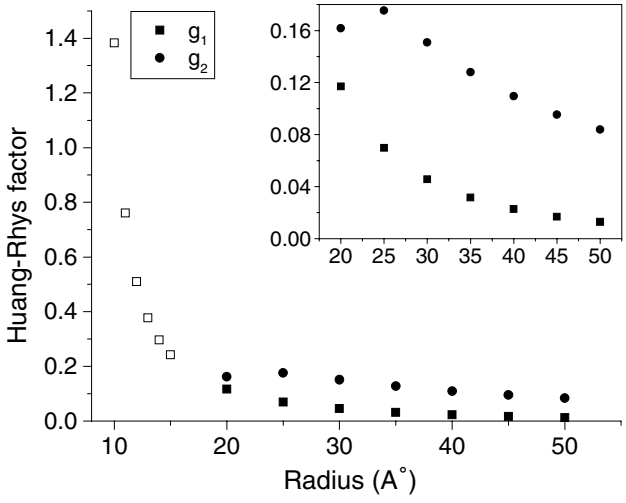

Fig. 2. The Huang–Rhys factors of small spherical GaAs/AlAs QDs obtained with Eq. (6). The results for larger QDs are magnified in the inset. The open squares represent results for the region where the effective mass approximation becomes questionable (see the text).

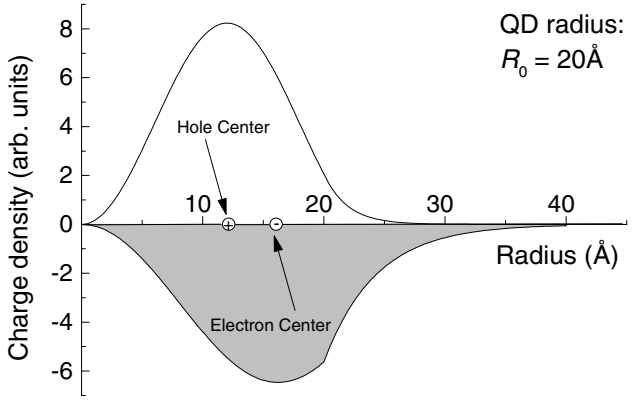

Fig. 3. The charge separation of small spherical GaAs/AlAs QDs with radius $R_0 = 20$ Å for the first EHP state induced by finite potential barriers. The plus and minus circle symbols indicate position of the center of positive and negative charges, respectively.

comes inadequate, the measured values range from 0.5 for small QDs (below 45 Å) [21] to 0.05 for larger QDs [22,23]. Given the simplicity of our model, we may extend the limit of calculation to excited states. Thus, the Huang–Rhys factor g_2 of D_0 is slightly larger than g_1 of A_0, mainly due to a larger charge separation for this excited state. On the other hand, for larger radii we obtain smaller values, close to the values obtained theoretically for excitonic states of spherical GaAs microcrystallites in [24].

According to [3], when a EHP recombination occurs, the intensity of the equilibrium PL spectrum can be characterized by the product of absorption coefficients, $I_{\mathrm{PL}}(\omega) \propto \omega^3 \alpha(\omega_{\mathrm{exc}})\alpha(\omega)/\omega_{\mathrm{exc}}$, where ω_{exc} is the frequency of the monochromatic incident radiation. Thus, with expression from Eq. (3) for the absorption coefficient, the PL intensity obtained by exciting to level $D_0 + i \cdot \mathrm{LO}$ $(i = 0, 1, 2, \ldots)$ and recording from the level $A_0 + j \cdot \mathrm{LO}$ $(j = 0, -1, -2, \ldots)$ is written as

$$
\begin{aligned}
I_{\mathrm{PL}}(\omega) \propto \sum_{i\geqslant 0, j\leqslant 0} & I_i\left(2g_2\sqrt{\overline{N}(\overline{N}+1)}\right) I_j\left(2g_1\sqrt{\overline{N}(\overline{N}+1)}\right) \\
& \times \exp\left[-\beta\hbar\left(\frac{(i+j)\omega_0}{2}+\omega_1\right)\right] \\
& \times \left[A_{110}^2 \mathrm{e}^{-(g_1+g_2)(2\overline{N}+1)}\left(\frac{\omega_1-\Delta_1+\mathrm{j}\omega_0}{\omega_2-\Delta_2-\mathrm{i}\omega_0}\right)^2\right. \\
& \times \delta(\omega_{\mathrm{exc}}-\omega_2+\Delta_2+\mathrm{i}\omega_0)\delta(\omega-\omega_1+\Delta_1-\mathrm{j}\omega_0) \\
& + A_{120}^2 \mathrm{e}^{-2g_2(2\overline{N}+1)}\left(\frac{\omega_2-\Delta_2+\mathrm{j}\omega_0}{\omega_2-\Delta_2-\mathrm{i}\omega_0}\right)^2 \\
& \left. \times \delta(\omega_{\mathrm{exc}}-\omega_2+\Delta_2+\mathrm{i}\omega_0)\delta(\omega-\omega_2+\Delta_2-\mathrm{j}\omega_0)\right].
\end{aligned}
\tag{7}
$$

According to the previous discussion regarding the energy-level distribution, the probability of a sequential relaxation process of EHP may be neglected for the range 10–32 Å at low temperatures, and, consequently, for this range, we may consider emission processes occurring from the EHP states. Figs. 4(a) and (b) show the absorption spectra obtained with Eq. (3) and the PL spectra obtained for a resonant excitation of the level D_0 for $R_0 = 25$ Å, in which the line shape has been modeled by Lorentzians with a width of 15 meV (a limited spectral resolution of experimental equipment is considered, see e.g. [3]). The familiar LO-phonon sidebands appear in both the absorption and PL spectra. As expected, the spectra have weak temperature dependence. The possibility of non-resonant excitations is reflected by the presence of the LO peaks on the positive side of the absorption spectrum. Weaker negative (positive) lines in the absorption (PL) spectra would disappear at zero temperature, and appear at temperatures where LO phononic population becomes significant. The nega-

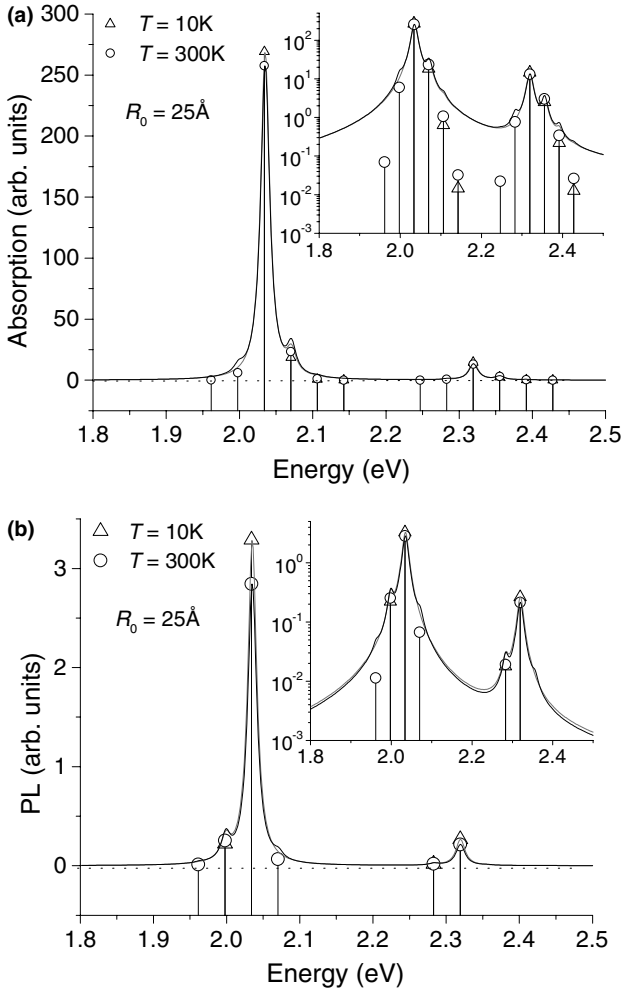

Fig. 4. The absorption (a) and PL (b) spectra of GaAs/AlAs QDs $R_0 = 25$ Å. The lines and their associated symbols represent the intensities, which are proportional to the factor of the Dirac delta functions from Eq. (3) for absorption and from Eq. (7) for PL. PL is obtained from resonance excitation, with $i = 0$, see the text. The insets show in detail the LO phononic progressions. The black (gray) lines are for the spectra at $T = 300$ K (10 K).

tive absorption sidebands implies a direct LO phonon–photon coupling, highly improbable as the particles have much different energies. Though possible, to our knowledge, such a process has not been observed experimentally. Thus, the real presence of negative absorption sidebands must be further analyzed by relaxation dynamics studies. On the other hand, the positive PL sidebands would involve a simultaneous relaxation-recombination process of LO phonon and EHP particles. Though, separately, the two processes have much different relaxation times, the obtained PL lines support formation of the EHP-polaron whose relaxation is a one-step process [25]. The PL spectral line shape has a form similar to that obtained from the experiments in [21–23], for InAs/GaAs self-assembled QDs. We perform calculations for different radii at $T = 10$ K (not shown in figures), and find that as the radii values are increased (20 Å/30 Å/50 Å), (i) the absorption strengths for level A_0 (D_0) increase (decrease), and the ratios for the 0 LO peaks are approximately 1/1.32/1.6 (3/1.69/1); (ii) the PL intensities for both A_0 and D_0 levels decrease, and the ratios for the 0 LO peaks are approximately 1/0.6/0.36 and 1/0.21/0.05, respectively.

In conclusion, an adiabatic treatment of the "bosonic pure EHPs carriers plus phonons" system yields a spectral function similar to the well-known adiabatic spectral function of fermions. The adiabatic approach is justified in characterizing the optical spectra of small spherical QDs, unless the optical levels are mixed with other (optical or dark) levels via phonons. The simple model of EHP within finite barrier potentials represents a useful tool in providing, within acceptable limits, the energy spectrum, the Huang–Rhys factor, and the description of the absorption and PL spectra of small spherical QDs. The adiabatic treatment of small spherical QDs, a case where the nonadiabatic effects can be neglected, yields Huang–Rhys factors larger by one to two orders of magnitude than those in the bulk phase. A quantitative analysis, which could predict accurately the magnitude of the EHP–phonon coupling, requires refined models for QDs.

Acknowledgment

This work is supported by the National Science Council of Taiwan.

References

[1] J.C. Marini, B. Stebe, E. Kartheuser, Phys. Rev. B 50 (1994) 14302.
[2] J. Zhao, S.V. Nair, Y. Masumoto, Phys. Rev. B 63 (2000) 33307.
[3] V.M. Fomin, V.N. Gladilin, J.T. Devreese, E.P. Pokatilov, S.N. Balaban, S.N. Klimin, Phys. Rev. B 57 (1998) 2415.
[4] K. Huang, A. Rhys, Proc. R. Soc. Lond. A 204 (1950) 406.
[5] S. Nomura, T. Kobayashi, Phys. Rev. B 45 (1992) 1305.
[6] E. Menéndez, C. Trallero-Giner, M. Cardona, Phys. Stat. Sol. (b) 199 (1997) 81.
[7] E. Hanamura, Phys. Rev. B 37 (1988) 1273.
[8] (a) For the fermionic adiabatic spectral function, see, e.g G.D. Mahan, Many-Particles Physics, Kluwer Academic/Plenum Publisher, New York, 2000, Section 4.3;
(b) S. Mukamel, Principles of Nonlinear Optical Spectroscopy, Oxford University Press, Oxford, 1995, p. 217;
(c) We may also select S.H. Lin, R. Alden, R. Islampour, H. Ma, A.A. Villaeys, Density Matrix Method and Femtosecond Processes, World Scientific Publishing, Singapore, 1991;
Yu.E. Perlin, Sov. Phys. Solid State 10 (1969) 1531;
Y. Jung, E. Barkai, R.J. Silbey, Chem. Phys. 284 (2002) 181.
[9] T.O. Cheche, M.C. Chang, unpublished.
[10] G. Bastard, Wave Mechanics Applied To Semiconductor Heterostructures, Halsted, New York, 1988.
[11] A. Davydov, Théorie du Solide, Mir, Moscow, 1980.
[12] T. Takagahara, Phys. Rev. B 47 (1993) 4569.
[13] D.V. Melnikov, W.B. Fowler, Phys. Rev. B 64 (2002) 245320.
[14] M. Grundmann, O. Stier, D. Bimberg, Phys. Rev. B 52 (1995) 11969.
[15] V.V. Mitin, V.A. Kochelap, M.A. Stroscio, Quantum Heterostructures, Cambridge University Press, Cambridge, 1999, p. 143, Figs. 4.2 and 4.10.
[16] P.C. Sercel, K.J. Vahala, Phys. Rev. B 42 (1990) 3690.
[17] K. Oshiro, K. Akai, M. Matsuura, Phys. Rev. B 66 (2002) 153308.
[18] K.J. Vahala, IEEE J. Quantum Electron. QE-24 (1988) 523;
M.P. Chamberlain, C. Trallero-Giner, M. Cardona, Phys. Rev. B 51 (1995) 1680.
[19] S. Schmitt-Rink, D.A.B. Miller, D.S. Chemla, Phys. Rev. B 35 (1987) 8113.
[20] H. Zhao, S. Wachter, H. Kalt, Phys. Rev. B 66 (2002) 085337.
[21] A. García-Cristóbal, A.W. Minnaert, W.M. Fomin, J.T. Devreese, A.Yu. Silov, J.E.M. Haverkort, J.H. Wolter, Phys. Stat. Sol. (b) 215 (1999) 331. Based on the Luttinger formalism, Garcia-Cristobal et al. are able to obtain Huang–Rhys factors one to two orders of magnitude larger than in the bulk using the adiabatic approach.
[22] M. Bissiri, G. Baldassarri Höger von Högersthal, A.S. Bhatti, M. Capizzi, A. Frova, P. Frigeri, S. Franchi, Phys. Rev. B 62 (2000) 4642.
[23] M. Bissiri, M. Capizzi, V.M. Fomin, V.N. Gladilin, J.T. Devreese, Phys. Stat. Sol. (b) 224 (2001) 639.
[24] Y. Chen, S. Huang, J. Yu, Y. Chen, J. Lumin. 60&61 (1994) 786.
[25] O. Verzelen, R. Ferreira, G. Bastard, Phys. Rev. Lett. 88 (2002) 146803.